RSC Pharmaceutics

ROYAL SOCIETY OF CHEMISTRY

PAPER

View Article Online
View Journal | View Issue

Cite this: *RSC Pharm.*, 2024, **1**, 357

Novel pH-sensitive gum ghatti-*cl*-poly(acrylic acid) composite hydrogel based on graphene oxide for metformin hydrochloride and sodium diclofenac combined drug-delivery systems†

Pragnesh N. Dave *[a] and Pradip M. Macwan[b]

Received 13th December 2023,
Accepted 3rd May 2024

DOI: 10.1039/d3pm00072a

rsc.li/RSCPharma

The objective of the present study was to synthesize pH-sensitive gum ghatti-*cl*-poly (acrylic acid)/GO hydrogels for the drug delivery and controlled combined release of metformin hydrochloride and sodium diclofenac. Gum ghatti (Gg) and acrylic acid (AA) were free radicals copolymerized using *N,N*′-methylenebisacrylamide (MBA) and tetramethyl ethylenediamine as cross-linkers and ammonium persulfate (APS) as an initiator. The structure and surface morphology of the composite hydrogel were determined using FTIR and SEM analyses, respectively. The FTIR studies confirmed the successful acrylic acid and graphene oxide grafting and drug binding onto the backbone of the synthesized hydrogel. Drug-release kinetics and mechanisms were investigated using zero- and first-order kinetic models as well as the Korsmeyer–Peppas model, Higuchi model, and Hixson–Crowell model. Drug-release experiments revealed the important characteristics related with physiologically expected pH levels, including a high release rate at pH 9.2. At pH 9.2, metformin HCl drug release increased from 4.68% to 37.46%, whereas sodium diclofenac release increased from 3.25% to 54.75%. However, at pH 9.2, both metformin hydrochloride and sodium diclofenac showed non-Fickian transport mechanisms. In summary, combining drugs may reduce the efficacy of a single medication while influencing metabolic rescue mechanisms.

1. Introduction

Hydrogels are 3D polymeric networks created through physical or chemical crosslinks that swell in water and can be synthesized from synthetic and natural polymers.[1,2] They provide unrivalled adaptability in terms of mechanical characteristics, swelling behavior, and biocompatibility. These qualities have led to their use in a wide range of applications, including tissue engineering, since the mechanical properties of hydrogels can be changed to fit a wide range of tissues,[3] drug delivery,[4] and filtration,[5,6] which use the physical and chemical restrictions of the mesh to encapsulate and regulate the release of a drug, nanoparticle, or other molecule.

In recent years, there has been an increasing interest in the development of stimulus-responsive hydrogels owing to their ability to significantly alter their volume and other parameters in response to a small change in external and internal stimuli, such as temperature, pressure, pH, and specific chemicals.[7] Because of the presence of reactive groups such as –OH, –COOH, $-NH_2$, $-CONH_2$, and $-SO_3H$, these materials are hydrophilic in nature and may absorb or retain substantial amounts of water; moreover, these hydrogels also contain bioactive molecules within their network. The development of improved drug delivery systems involves the use of cross-linked hydrogels that are non-toxic, biodegradable, and renewable in nature, as well as having a high water absorbency.[8,9] Natural polysaccharide-based hydrogels have features that allow them to be employed as drug carriers as well as in tissue engineering, wound dressing, waste water treatment[10–12] and other applications.[13–19]

The use of multiple drugs, or polypharmacy, often leads to drug–drug interactions, which may enhance drug-related toxicity in patients. It is true that any drug before being marketed has to pass through different phases of clinical trials in order to verify the safety and efficacy of the therapeutic agent in humans. However, even the stringent inclusion criteria in clinical trials often fail to reflect the real-world scenario. The scientific evaluation of drug–drug interactions in the real context of polypharmacy and comorbid conditions is very important to maximize the therapeutic outcome. However, to date, very few studies have been conducted to evaluate the

[a]*Department of Chemistry, Sardar Patel University, Vallabh Vidyanagar-388 120, Gujarat, India. E-mail: pragnesh7@yahoo.com*
[b]*B. N. Patel Institute of Paramedical & Science (Science Division), Sardar Patel Education Trust, Bhalej Road, Anand – 388001, Gujarat, India*

† Electronic supplementary information (ESI) available. See DOI: https://doi.org/10.1039/d3pm00072a

effect of individual drugs in a situation of concomitant drug used in comorbid situations.[20]

Previously, a novel gum ghatti-*cl*-poly(NIPAm-*co*-AA) composite hydrogel with different graphene oxide (GO) concentrations was synthesized through graft-copolymerization by our group[21] to investigate the effective complex formation and to analyze the type and intensities of complexes that may occur by the interactions of metformin and sodium diclofenac at different pH values.

The usage of natural polysaccharides in drug delivery is a topic of powerful research because of their biocompatibility and biodegradability. Gum ghatti (Gg) is a high-molecular-weight anionic polysaccharide derived from the *Anogeissus latifolia* plant in the *Combretaceae* family. D-Glucuronic acid, D-xylose, D-mannose, D-galactose, and L-arabinose make up the main structure of gum ghatti. Because of its thickening and emulsifying qualities, gum ghatti is frequently utilized in the paper, pharmaceutical, and food sectors. It is especially used in the development of pharmaceutical formulations as a sustained-release, matrix-forming, film-forming, and mucoadhesive polymer.[22] Gg is a naturally occurring plant polysaccharide that comprises alternating 4-*O*-substituted and 2-*O*-substituted alpha-D-mannopyranose units and chains of 1–6 linked β-D-galactopyranose units with side chains that are most commonly single L-arabinofuranose residues.[23] In our previous work,[23] the probable structure of gum ghatti was discussed. Poly(acrylic acid) is an anionic polymer that is commonly employed in the creation of various dosage forms, particularly pH-sensitive hydrogels. Each monomer unit in the poly(acrylic acid) chain has one carboxyl group. Poly(acrylic acid) dissociation increases with the increasing medium pH (due to the carboxyl group). Poly(acrylic acid) is used in a variety of medical and pharmaceutical applications, including bioadhesives, drug-delivery systems, oral suspensions, and as a dispersion agent in food processing and cosmetic goods.[24] The APS–TEMED redox pair is a commonly used initiator system for gel-formation reactions. TEMED molecules generate free radicals, resulting in a three-fold increase in the polymerization rate compared to the absence of an accelerator.[25] Tetramethylethylenediamine (TEMED) is widely used with APS as a redox pair to initiate the polymerization of acrylic acid hydrogels under mild circumstances and has been introduced for the preparation of poly(acrylic acid)/GO hydrogels.

Sharma *et al.*[26] successfully used a free-radical-polymerization technique to create conducting hydrogels based on gum ghatti. The grafting and crosslinking improved the samples' thermal stability, according to thermal analysis. Amoxicillin trihydrate and paracetamol could be released from hydrogels more readily at pH 9.2 than at pH 2.4 or pH 7. For both drugs, the conducting hydrogel proved to be an effective drug-delivery method in alkaline pH. According to Ali *et al.*,[27,28] adding GO to the hydrogel network improved its mechanical characteristics, self-healing abilities, drug-entrapment effectiveness, and ensured the controlled release of the entrapped drug. We observed how GO affected the hydrogel's properties through studies of its self-healing qualities, swelling behavior, degradation, and by tensile and compressive tests, and investigation of its rheological behavior, and *in vitro* drug-release behavior. Our findings suggested that the hydrogel, which is a self-healing nanocomposite, could serve as a platform for drug delivery at pH 7.4. Kaith *et al.*[29] investigated the *in situ* release of cetirizine dihydrochloride using a gum tragacanth–acrylic acid hydrogel at 37 °C and at pH levels of 2.0, 7.0, and 9.2. A fractional factorial design was used to screen a variety of process variables, including solvent, temperature, pH, treatment time, initiator molar ratio, monomer concentration, and cross-linker. However, at pH 9.2, a non-Fickian mechanism was observed. Similarly, colon-specific drug-delivery systems for amoxicillin trihydrate and paracetamol were developed using crosslinked hydrogels derived from Gg at pH levels of 2.0, 7.0, and 9.2. A two-step aqueous polymerization was used to create an electrically active hydrogel interpenetrating network (IPN) composed of Gg, poly(acrylic acid) (AA), and polyaniline. The release of amoxicillin trihydrate and paracetamol increased with increasing the pH. The highest release was observed at basic pH for both Gg-*g*-poly(AA) and Gg-*g*-poly (AA-IPN-ANI) with amoxicillin trihydrate and paracetamol.[26] Several other hydrogel systems have been studied synthesized by different polymerization techniques with different drugs for drug-delivery systems (Table S1†).

For instance, silver nanoparticles were synthesized using *Saccharum officinarum* plant extracts, resulting in a CH-Ag bionanocomposite. The method was environmentally friendly. The AgNPs ranged in size from 50 to 100 nm. The CH-Ag bionanocomposite was evaluated for different drug-release profiles, including itraconazole, at various pH levels (pH 2, 7, and 9). The results showed sustained drug release from the CH-Ag bionanocomposite. The highest drug release occurred at pH 7, followed by pH 9.2 with the lowest release.[30] The drug quercetin (QC), which has antioxidant, antiviral, and anticancer properties, was loaded into a new nanocarrier based on a hydrogel nanocomposite containing chitosan (CS), carboxymethyl cellulose (CMC), and carbon nanotubes (CNTs). Furthermore, the use of CNTs increased drug loading by 48.0% and encapsulation by 86.5%. Moreover, in the study, the cytotoxicity of the nanocarriers with QC was measured using MTT analysis, and by examining the results, it was discovered that CS/CMC/CNTs/QC had a significantly higher cytotoxicity against the MCF-7 cell line than free QC. The CNT nanoparticles had an inhibiting impact and improved the release behavior of the nanocarriers. The controlled release of QC from the CS/CMC/CNTs/QC complex amplified cellular apoptosis while diminishing cell viability. Furthermore, the late apoptotic cell ratio observed in CS/CMC/CNTs/QC samples surpassed that of cell size samples in the apoptosis assay, indicating enhanced efficacy, which could be attributed to the controlled and slow release of QC from CS/CMC/CNTs/QC.[31] Various nanodelivery systems have been used to deliver CRBP (1,1-cyclobutyldicarboxylate), including polymer-based nanocarriers, protein nanoparticles, lipid-based nanoparticles (liposomes and solid lipid nanoparticles), silica-based nanostructures, and carbon nanoparticles. Future prospects for CRPB delivery include

enhanced targeting, combination therapies, personalized medications, image-guided delivery, and smart drug delivery. Specific triggers (*e.g.*, pH, temperature, enzyme activity) at the tumor site could improve targeting and reduce off-target effects.[32] Several hydrogel systems have been studied for drug delivery with varied applications (Table S2†).

Additionally, because of its hydrophilic oxygen-containing groups, GO can be easily removed and steadily distributed as single-layer sheets in an aqueous solution, which is advantageous for the preparation of mechanically strong nanocomposite hydrogels. By interacting physically and chemically with the hydrophilic polymer matrices, the oxygen-containing functional groups enable the graphene oxide (GO) nanosheets to greatly improve the mechanical performance. With reference to the aforementioned problem statement, an attempt was made to use *N,N*′-methylene-bis-acrylamide (MBA) and ammonium persulfate (APS) as a cross-linker-initiator system for the free radical copolymerization of hydrogel composites based on gum ghatti with an interpenetrating network under vacuum. Fourier transform infrared (FTIR) spectroscopy and scanning electron microscopy (SEM) methods were used to characterize the structures of the candidate polymers.

Graphene oxide (GO) is a 2D water-soluble graphene derivative having oxygen-containing groups, such as hydroxyl, carboxylic, and carbonyl, at its edges and epoxy on the surface.[33] Because of these functional groups, GO is a promising choice for increasing the drug-adsorption capabilities and mechanical strength of polymeric hydrogels. GO has been identified as a potential molecule for drug administration due to its high dispersibility in aqueous media, low toxicity, wide specific surface area, and strong electrostatic interactions with various adsorbates.[34] Yang *et al.*,[35] for example, investigated the loading and release performance of doxorubicin hydrochloride on GO, and discovered that the weight ratio of the loaded medication on to the GO carrier may approach 200%. Zhang *et al.*[36] sought to functionalize GO with folic acid and sulfonic acid groups in order to improve its physiological stability and cell-targeting capabilities. Furthermore, the presence of functional groups such as hydroxyl, carboxylic, and epoxy resulted in graphene oxide's high compatibility with diverse systems, such as biomolecules[37] and organic and inorganic materials,[38] *via* covalent and non-covalent interactions.[39,40] Applying a polymer coating of GO eliminates the size and form constraints of GO, optimizing its efficiency for drug-delivery applications.[41,42]

Metformin HCl (Fig. 1), a biguanide derivative, is the chosen first-line oral blood glucose-lowering medication for type 2 diabetes management. It has three basic functions: reducing sugar absorption in the small intestine, stopping the liver from excreting more glucose into the blood, and eventually supporting the body in using natural insulin properly. As a result, it reduces endogenous glucose synthesis while causing no obvious hypoglycemia. However, because it is hydrophilic, it is only partly and slowly absorbed by the gastrointestinal system, resulting in a relatively poor bioavailability (50%–60%).[43,44] Furthermore, because metformin HCl has a very short half-life (2–4 h), frequent administration of the drug is required for effective treatment. Furthermore, metformin HCl drugs may increase the occurrence of gastrointestinal symptoms, such as increased flatulence, stomach discomfort, anorexia, cramps, nausea, vomiting, diarrhea, and weight loss, all of which can contribute to patient noncompliance with their treatment. The development of a metformin HCl sustained-release formulation may provide a solution to the aforementioned limitations by improving gastrointestinal tolerability, and permitting once-daily dosage, therefore increasing patient compliance.[45]

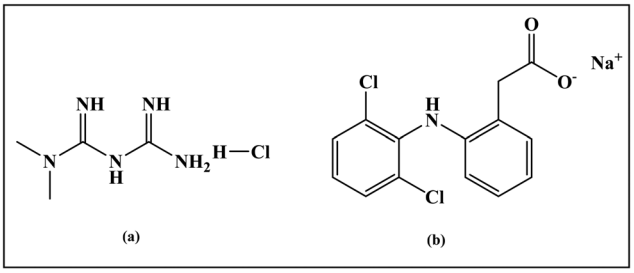

Fig. 1 Chemical structures of the drugs: (a) metformin hydrochloride and (b) sodium diclofenac.

Diclofenac sodium is a nonsteroidal anti-inflammatory, analgesic and antipyretic drug (NSAID) (Fig. 1).[46] It is a sodium salt of an aminophenyl acetic acid that is rapidly absorbed after oral administration, with a biological half-life of 1–2 h and a high solubility above pH 5. Although this medicine is frequently used in the treatment of tendinitis, rheumatoid arthritis, osteoarthritis,[2] and ankylosing spondylitis, features such as a short half-life and certain adverse effects limit its clinical use. The most frequent adverse effects include stomach discomfort, gastritis, peptic ulcer, and bleeding.[47] Recent studies have been conducted to increase drug release, such as the use of tableted microspheres, acetate butyrate microparticles (a kind of polymer), and nanoparticles. Studies utilizing biomaterials as drug-release carriers have demonstrated effectiveness in overcoming such issues and improving the drug-release rate and targeting.[26]

The main objective of this study was to investigate complex formation and analyze the types and intensities of complexes that can result from metformin and diclofenac interactions and also to develop a pH-sensitive polymeric network of hydrogels *via* a free-radical-polymerization technique for the controlled delivery of metformin HCl and sodium diclofenac drugs. Such a polymeric network may be able to overcome the complications related with conventional systems and may help to keep the drug steady-state plasma concentration, allowing decreasing the dose frequency due to the larger loading ability, ultimately improving patient compliance. To address these issues, an attempt was made to develop hydrogel composites based on gum ghatti with an interpenetrating network through the use of free radical copolymerization and a cross-linker-initiator system, which included tetramethylethylenediamine (TEMED) as an initiator, *N,N*′-methylene-bis-

acrylamide (MBA), and APS. Additionally, using sodium diclofenac and metformin hydrochloride as model drugs, the release profile of the synthesized hydrogels was investigated. Kinetic analysis was done for release of the drugs sodium diclofenac and metformin hydrochloride from the synthesized hydrogels. To make the current study more informative, an attempt was made to understand the development, characteristics, and uses of hydrogels based on natural polysaccharides. The synthesized hydrogels had various functional groups, like –OH, –COOH, and –CH, which helped the facile loading and sustained release of metformin hydrochloride and sodium diclofenac (SD) model drugs from the synthesized hydrogels. This new GO modification strategy can enable the creation of high-performance nanocomposites for biomedical engineering applications, including artificial tissue generation.

2. Experimental

2.1. Chemicals and reagents

Gum ghatti (Loba Chemie, Mumbai, India) (Table S3† displays the general features of gum ghatti), acrylic acid (AA) (Sigma Aldrich, 99%), ammonium persulfate (APS) (Merck, ≥98.5%), tetramethyl ethylenediamine (TEMED), and *N,N*'-methylenebisacrylamide (MBA) were purchased from Loba Chemie (Mumbai, India). Graphene oxide was purchased from Sigma Aldrich (Munich, Germany). All the materials used in the present study were of reagent grade. Metformin hydrochloride was purchased from Himedia (CAS no. 1115-70-4). Sodium diclofenac was supplied by Sigma Aldrich (SD) (CAS no. 15307-79-6). Throughout the experiments, triple distilled water was used.

2.2. Preparation of gum ghatti-*cl*-poly(acrylic acid)/GO

Hydrogels composed of gum ghatti-*cl*-poly(AA) and gum ghatti-*cl*-poly(AA)/GO were synthesized by free radical polymerization. First, GG (0.5 g) was dissolved in 10 mL deionized water in a 100 mL beaker. Then 0–5 mg of GO was dispersed into this mixture and then the solution was sonicated for 40 min at room temperature by using an ultrasonicator, and this mixture was then agitated by a mechanical stirrer (250 rpm). Thereafter, 50 mg of *N,N*'-methylene bis-acrylamide (MBA), used as a cross-linker, was added to the beaker followed by 1 mL of AA, and 10 mL of deionized water. The beaker was then heated to 60 °C for 20 min. Free radicals were produced using ammonium persulfate (APS) (50 mg) as an initiator and 0.05 ml of tetra methyl ethylene diamine (TEMED) as an accelerator. The preliminary signal of gel formation appeared after 25 min. The reaction was then continued for 3 h in an hot air oven for completion of the polymerization process.[48,49] The non-reactive ingredients were removed from the hydrogels by repeatedly washing them with deionized water. The hydrogel was allowed to gradually dry for 48 h at 50 °C. The above-mentioned method was used to create gum ghatti-*cl*-poly(AA) hydrogels without the need for GO.[50] The material data sheet is presented in Table 1. The possible mechanism for the synthesized hydrogel is depicted in Scheme 1.

The synthesis of the gum ghatti and acrylic acid hydrogel by free radical polymerization using APS (ammonium persulfate) and a cross-linker occurred by the following mechanism:

2.2.1. Generation of free radicals. Ammonium persulfate (APS) was used as an initiator in this reaction. APS separates into two sulfate radicals, which are highly reactive free radicals. This reaction can be symbolized as below:

$$(NH_4)_2S_2O_8 \rightarrow 2NH_4^+ + 2SO_4^{\bullet}$$

2.2.2. Initiation. The sulfate radicals attack the double bond of the acrylic acid, triggering the polymerization reaction. This creates a new free radical on the acrylic acid monomer:

$$SO_4^{\bullet} + CH_2 = CHCOOH \rightarrow (CH_2\text{-}CHCOOH)^{\bullet}$$

2.2.3. Propagation. The new free radical on the acrylic acid monomer attacks another monomer, resulting in a chain reaction. This procedure is repeated till the chain has reached a certain length:

$$(CH_2\text{-}CHCOOH)^{\bullet} + CH_2 = CHCOOH \rightarrow (CH_2\text{-}CHCOOH)_2^{\bullet}$$

2.2.4. Crosslinking. To form a hydrogel, a cross-linker is added to the reaction mixture. The cross-linker contains multiple functional groups that can react with the free radicals on the polymer chains, forming covalent bonds between the chains. This process is called crosslinking, and it leads to the formation of a three-dimensional network, resulting in the hydrogel.

2.2.5. Termination. The polymerization reaction is terminated by the combination of two free radicals or by the reaction with a chain transfer agent.

2.2.6. Overall reaction

$$(CH_2 = CHCOOH)_n + \text{Cross-linker} \rightarrow \text{Gum ghatti and acrylic acid hydrogel}$$

. Gum ghatti is a polysaccharide that is commonly used to improve the rheology of hydrogels. Gum ghatti molecules

Table 1 Composition and various characteristic parameters of the gum ghatti-*cl*-poly(AA)/GO (GGAAGO) nanocomposites hydrogels

Hydrogel	Gum ghatti (g)	AA (ml)	APS (g)	MBA (g)	TEMED (ml)	GO (mg)	H_2O (ml)
GGAAGO-0	0.5	1	0.05	0.05	0.05	0	10
GGAAGO-1	0.5	1	0.05	0.05	0.05	1	10
GGAAGO-2	0.5	1	0.05	0.05	0.05	2	10
GGAAGO-3	0.5	1	0.05	0.05	0.05	3	10
GGAAGO-4	0.5	1	0.05	0.05	0.05	4	10
GGAAGO-5	0.5	1	0.05	0.05	0.05	5	10

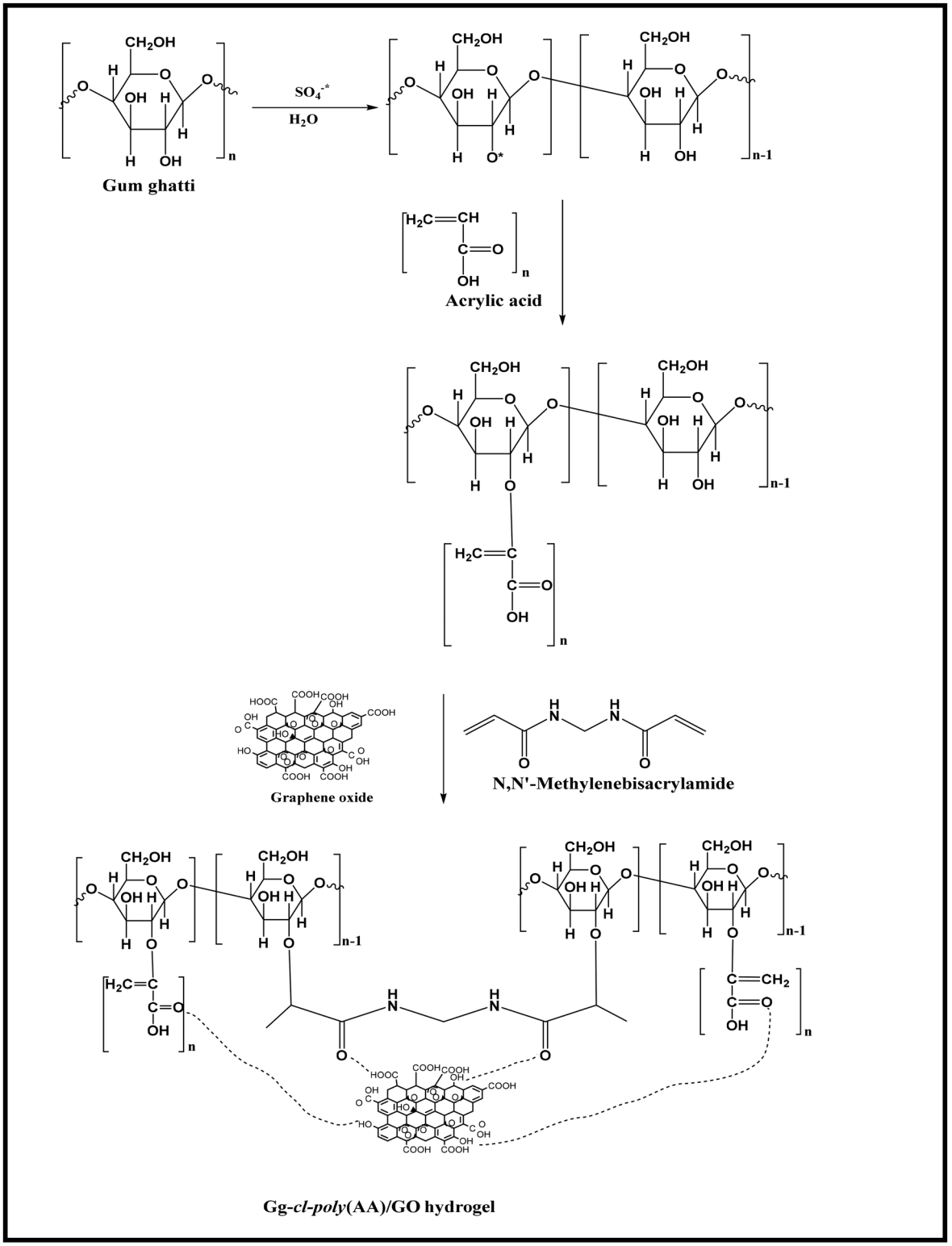

Scheme 1 Possible and proposed mechanism for the addition of graphene oxide (GO) on the Gg-*cl*-poly(AA) hydrogel matrix.

interact with polymer chains and cross-linkers, influencing the hydrogel's final structure and properties. The specific cross-linker used in the reaction varies according to the application and desired hydrogel properties. The cross-linker's structure is determined by the type and number of functional groups present. The cross-linker may contain two or more functional groups that can react with the polymer chains' free radicals to form covalent bonds. In general, the synthesis of the gum

ghatti and acrylic acid hydrogel by free radical polymerization with APS and a cross-linker involved the formation of a polymer chain *via* acrylic acid monomer polymerization, followed by polymer chain crosslinking to form a hydrogel. The gum ghatti molecule in the reaction mixture helped shape the hydrogel's final structure and properties.

2.3. Characterization of the hydrogel

2.3.1. Fourier transform infrared spectroscopy (FTIR). The grafting of acrylic acid (AA) on to the gum ghatti chains and the addition of graphene oxide (GO) in the gum ghatti-based hydrogels were characterized using Fourier transmission infrared spectroscopy (FTIR). The FTIR spectra of gum ghatti, graphene oxide, and the drug-loaded GGAAGO-0 and GGAAGO-3 were obtained using KBr pellets in an MB 3000 FTIR spectrometer (ABB Pvt. Ltd, Germany). The spectra were captured between 4000 and 400 cm^{-1} wavelengths.

2.3.2. Surface morphological study (SEM). The morphology of particles was studied by SEM analysis on a scanning electron microscope. In this method, a sample is scanned using a high-intensity electron beam. A Field Emission Gun Nano Nova Scanning Electron Microscope (FEG-SEM) 450 system with EDAX was used to analyze the hydrogels. For sample analysis, the magnification levels ranged from ×25 to ×10 000.

2.4. Drug-loading study

2.4.1. Loading of metformin and sodium diclofenac onto the hydrogel. The model drugs sodium diclofenac and water-soluble metformin were introduced into the hydrogel using a swelling-diffusion method. A 100 mL solution of metformin (1.0 mg mL^{-1}) and sodium diclofenac (1.0 mg mL^{-1}) was poured on to the dried hydrogels (1.0 g), and they were then incubated at 37 °C for 24 h. After being taken out of the solutions, the composite hydrogels were rinsed with deionized water and dried in an oven at 50 °C to a consistent weight. Using a UV-Visible spectrophotometer, the amounts of metformin and sodium diclofenac were determined (Shimadzu-1800). The drug-entrapment efficiency (EE) of the hydrogel was determined using eqn (1) shown below:

$$\mathrm{DL}(\%) = \left(\frac{W_D}{W_0}\right) \times 100 \quad (1)$$

where W_D is the total amount of drug in solution after loading and W_0 is the total amount of drug in solution before loading.

2.4.2. *In vitro* drug-release study. The release profiles of the model drugs from the drug-loaded hydrogel (powder type) were studied in distilled water, and at pH 1.2 buffer (simulated gastric fluid), at pH 7.4 buffer (simulated intestinal fluid), and pH 9.2 (borate). The calibration curves of the drugs were prepared in distilled water, in pH 1.2 buffer, in pH 7.4 buffer, and in pH 9.2 buffer solutions at 232 nm for metformin and at 276 nm for sodium diclofenac using a UV-Visible spectrophotometer (Shimadzu-1800). The release experiments were performed by immersing the drug-loaded hydrogels in 100 mL PBS buffer (pH 7.4), HCl (pH 1.2), and borax (pH 9.2) solutions. The release studies were performed at a physiological temperature of 37 °C in an incubator at 100 rpm. A small volume of the release medium (5.0 mL) was withdrawn at scheduled time intervals in order to determine the drug concentration using the UV-Visible spectrophotometer and an identical volume of fresh medium was added to replace this.

2.4.3. Mechanism of drug release. The release data was fitted by the well-known Korsmeyer–Peppas equation shown below to describe the drug-release process:[51]

$$\frac{M_t}{M_\infty} = kt^n \quad (2)$$

where k is a release rate constant typical of the structure and geometry of the drug-delivery device, n is the diffusion exponent characteristic of the release mechanism, and M_t/M_∞ is the proportion of the drug released at time 't'.[52–54] The values of n and k were obtained from the slope and intercept of the $\log M_t/M_\infty$ plot and the $\log t$ plot, respectively. Depending on the relative rates of water diffusion into the polymer matrix and rate of polymer chain relaxation, there are three different ways that drugs can be released from drug-loaded polymers. For the samples, n = 0.89 related to case II diffusion (the release mechanism was relaxation controlled), n = 0.45 was related to Fickian diffusion (the release mechanism was diffusion controlled), and n between 0.45–0.89 was related to non-Fickian diffusion[2] (a mixture of Fickian diffusion and polymer chain relaxation).

2.4.4. Kinetics of drug release. The best fit of the curves to several kinetic models, including the zero-order model (eqn (3)), first-order model (eqn (4)), Higuchi model (eqn (5)), Korsmeyer–Peppas model (eqn (6)), and Hixson–Crowell model (eqn (7)), was used to determine the kinetics of drug release from the hydrogel. The relevant equations are given below.

$$\frac{M_t}{M_\infty} = k_0 t \quad (3)$$

$$\log\left(\frac{M_t}{M_\infty}\right) = k_1 t \quad (4)$$

$$\left(\frac{M_t}{M_\infty}\right) = k_2 t^{\frac{1}{2}} \quad (5)$$

$$\left(\frac{M_t}{M_\infty}\right) = k_3 t^n \quad (6)$$

$$\sqrt[3]{M_0} - \sqrt[3]{M_t} = k_4 t \quad (7)$$

In the above stated models M_t/M_∞ is the cumulative fraction of drug release, t is the release time, n is the release exponent, M_0 is the amount of drug loaded in hydrogel, M_t is the amount of drug release at time t, and k_0, k_1, k_2, k_3, and k_4 are the release rate constants.[55]

3. Results and discussion

3.1. FTIR spectroscopy

As shown in Fig. 2, peaks at 3510, 2980, 1710, 1610, 1375, 1240, and 1050 cm^{-1} were found in the GO. These could be attributed to the bending and stretching vibrations of O–H, C═O stretching of carboxylates and conjugated carbonyls, and aromatic C═C, C–O–C, CO–H, and C–O stretching vibrations, respectively, while the peaks at 957 and 670 cm^{-1} appeared to be due to C–H stretching vibrations.[56] This result showed the presence of hydroxyl and oxygen groups on the GO surface.[57]

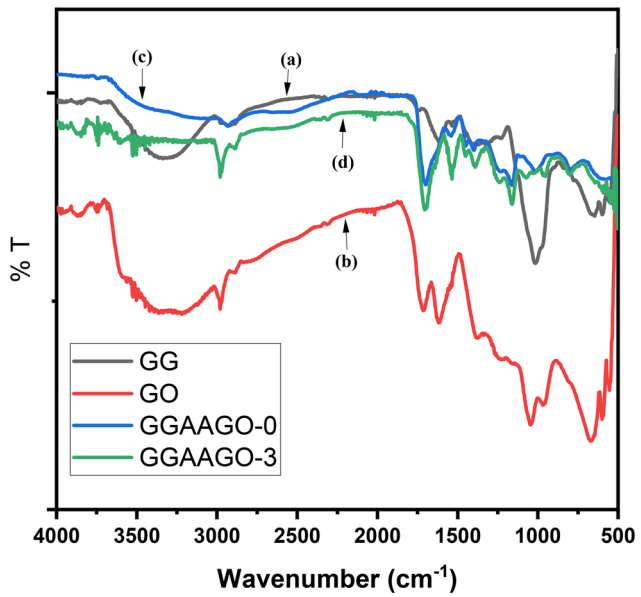

Fig. 2 FTIR spectra of (a) pure gum ghatti, (b) pure graphene oxide (GO), (c) the pure GGAAGO-0 hydrogel, and (d) the GGAAGO-3 hydrogel sample with 3 mg of graphene oxide.

The successful functionalization of GO nanosheets with gum ghatti-*cl*-poly(AA) was supported by the presence of the above-mentioned FTIR peaks in the spectrum of gum ghatti-*cl*-poly(AA)/GO. Fig. 2 shows the FTIR spectra of GG, GO, gum ghatti-*cl*-poly(AA), and gum ghatti-*cl*-poly(AA)/GO. The following peaks were observed in the FTIR spectrum of GG: a broad peak at 3215 cm^{-1}, which was assigned to O–H stretching vibration;[58] a band at 1310 cm^{-1}, ascribed to O–H bending (in plane) or C–H bending; and a strong band at 1015 cm^{-1} assigned to C–O stretching vibration.[59] The low-intensity band at 631 cm^{-1} was associated with C–O or O–H bending vibrations (out of plane). The presence of an amide functional group in GG was shown by the appearance of a band at 1612 cm^{-1}.[60] The stretching vibration of the carbonyl group in carboxylic acid appeared at 1710 cm^{-1} and the peak of symmetrical vibration of COOH at 1384 cm^{-1} confirmed the formation of the gum ghatti-*cl*-poly(AA) hydrogel,[61] which was also supported by the absence of a peak at 1534 cm^{-1}, which would be a characteristic peak of C═C. This demonstrated that the C═C bond in AA was changed to a C–C bond, which resulted in the formation of PAA in the hydrogel. As shown in Fig. 2, the FTIR spectrum of gum ghatti-*cl*-poly(AA)/GO displayed new absorption bands at 2915, 1710, and 1161 cm^{-1}, assigned to the stretching vibrations of C–H, C═O, and C–O,[4] compared to that of GO, indicating that PAA was successfully grafted onto GO.[62]

3.2. Scanning electron microscopy (SEM) study

SEM was used to examine the characteristics of the gum ghatt-*cl*-poly(acrylic acid) and gum ghatt-*cl*-poly(acrylic acid)/GO hydrogel. As shown in Fig. 3 (Fig. 3a and b), the surface morphology of both the hydrogel and its nanocomposite was essentially peeled smooth with a rough, irregular surface morphology. The white layer on the peeling smooth was created by the impregnation of GO within the gum ghatt-*cl*-poly(acrylic

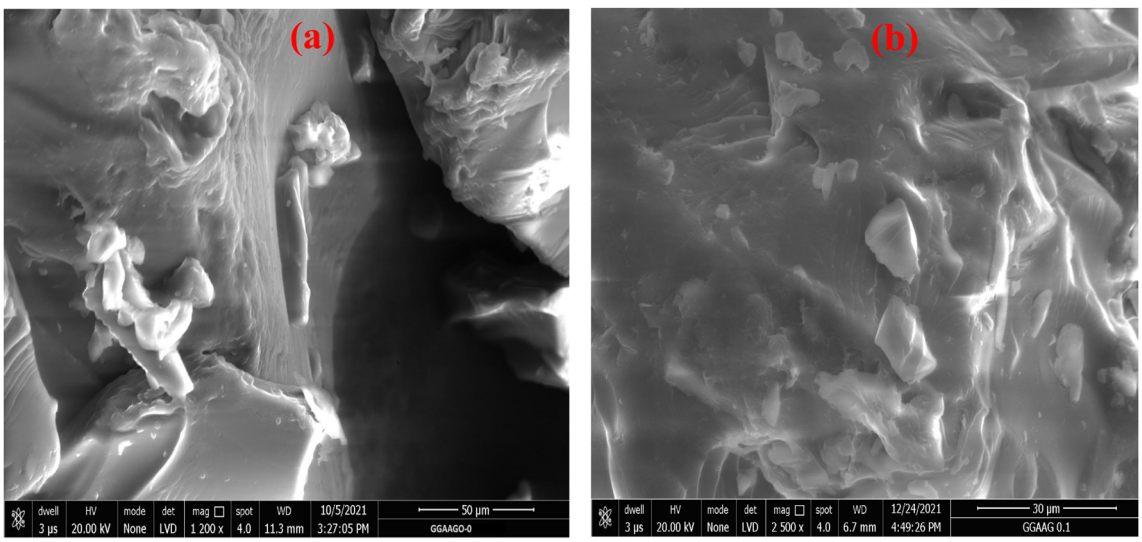

Fig. 3 Morphological analysis of (a) GGAAGO-0 (50 µm) and (b) GGAAGO-3 (30 µm) hydrogels.

acid) hydrogel polymer matrix (Fig. 3b); while the shape was completely different from that of the hydrogel (Fig. 3a).[63]

The SEM images confirmed that the synthesized polymeric network exhibited an irregular and porous fibrillar structure. These pores within the network play a crucial role in enabling the passage of water or other fluids. Furthermore, these pores also serve as the sites where the hydrophilic groups of the polymeric network interact with external stimuli. The presence of this porous structure on the surface of the polymeric network supports its high swelling tendency. The interconnected pores provide ample space for the absorption and retention of water or other fluid environments. This characteristic is essential for hydrogels intended for drug-delivery applications, as it allows for the efficient diffusion of drugs and promotes sustained release. The SEM images provide visual evidence of the porous and interconnected structure of the Aloe vera–AAm polymeric network, confirming its potential as a suitable material for applications such as drug-delivery systems and other biomedical applications.[64]

3.3. *In vitro* drug-release study

3.3.1. Effect of pH on metformin HCl drug release. The effect of pH on the metformin drug-release behavior through Gg-*cl*-poly(AA) and Gg-*cl*-poly(AA)/GO was investigated. From Fig. 4, it is apparent that for the hydrogels GGAAGO-0, GGAAGO-1, and GGAAGO-3, the cumulative drug release was about 3.36%, 7.17%, and 4.68% at pH 1.2; while for similar hydrogel samples, the drug release was found to be 30.98%, 29.85%, and 35.64% in more basic media at pH 7.4, and 34.46%, 39.78%, and 37.46% at pH 9.2 (Table 2). It is thus apparent from Table 2 that the release profile of metformin hydrochloride and sodium diclofenac drugs was greater at pH 9.2 (the same pH as colonic fluids) compared to that at pH 1.2

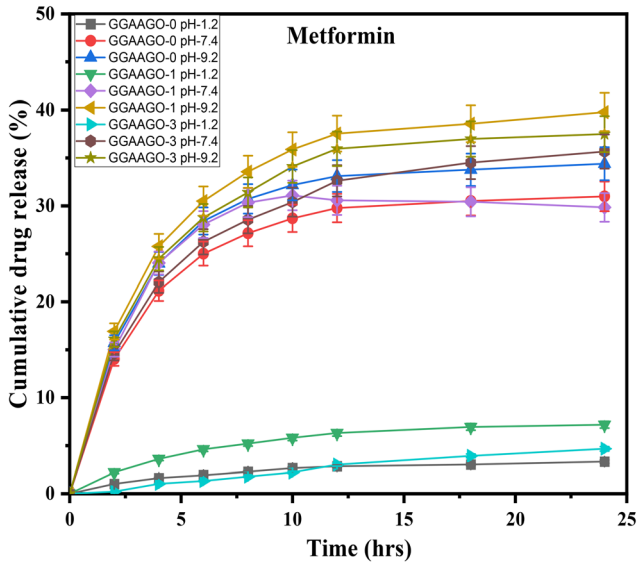

Fig. 4 Plots of cumulative drug release against time (hours) for metformin HCl-loaded GGAAGO-0, GGAAGO-1, and GGAAGO-3 hydrogels at pH 1.2, pH 7.4, and pH 9.2 and at 37 °C.

Table 2 Drug release (in percentage) from the hydrogel samples at pH 1.2, pH 7.4, and pH 9.2 at 37 °C

	Drug release (in %) at		
Hydrogels Metformin HCl	pH 1.2	pH 7.4	pH 9.2
GGAAGO-0	3.36 ± 2.2	30.98 ± 2.5	34.46 ± 1.8
GGAAGO-1	7.17 ± 2.0	29.85 ± 2.0	39.78 ± 1.7
GGAAGO-3	4.68 ± 1.2	35.64 ± 1.5	37.46 ± 2.1
Sodium diclofenac			
GGAAGO-0	3.66 ± 2.1	41.99 ± 1.9	54.97 ± 2.0
GGAAGO-1	3.56 ± 2.0	50.39 ± 1.8	61.56 ± 1.8
GGAAGO-3	3.25 ± 2.1	53.90 ± 1.5	54.75 ± 2.0

and pH 7.4. This means that the crosslinked hydrogels based on Gg are viable drug-delivery devices for colon-targeted drug-delivery systems.[65] Thus, it can be said that the synthesized hydrogels can potentially be used in the fabrication of controlled drug-delivery devices, where quick release of the drug is desired initially and sustained release thereafter.[26]

Fig. 4 shows the metformin hydrochloride release profile of the hydrogels at three different pH conditions: 1.2, and 7.4, 9.2. As can be seen in Fig. 4, the cumulative release increased rapidly with time (hours) and then reached an equilibrium value after a certain time. The equilibrium value was the highest at pH 9.2 and the lowest at pH 1.2. The initial slope of the curve, which is a measure of the release rate, was highest at pH 9.2 and lowest at pH 1.2. It was observed that the mechanism of metformin hydrochloride release from the as-prepared hydrogels was dependent on pH: at acidic and neutral pH's, the prevalent mechanism was diffusion, while at pH 9.2, the diffusion and chain relaxation were concomitantly important for the metformin hydrochloride diffusion. Some erosion of the polymeric matrix also helps to increase the release under alkaline conditions. The main findings are associated with the chemical structure of the hydrogels and the ionization of the carboxylic groups.

These results may be due to the fact that in acidic conditions, the hydrogel shrinks and the pore size drops, and so the drug release is hindered. In basic conditions, on the other hand, the hydrogel swells and the pore size upsurges, enabling the release of drugs.[66] This is due to the fact that at lower pH the $-COO^-$ groups are sheltered by H^+ ions and different polymer chains do not become so far apart from each other due to the least repulsion. Because of this, the polymer matrix remains in a collapsed state. On the other hand, at higher pH these partially ionized $-COO^-$ groups are the least sheltered and extreme repulsions between different polymeric chains exist, resulting in greater swelling of the matrix with increased fluid intake and hence increased drug diffusion.[26]

Metformin, an inhibitor of complex-I of the respiratory chain, has been shown in studies to inhibit some brain tumor initiating cells (BTICs), though at too high a dose for clinical use. As a result, we investigated whether combining metformin and diclofenac, a nonsteroidal anti-inflammatory drug (NSAID) known to inhibit glycolysis by interfering with lactate

efflux, would have additive or even synergistic effects on BTICs (BTIC-8, -11, -13, and -18) and tumor cell (TC) lines (TCs, U87, and HTZ349). The functional effects, such as proliferation and migration, metabolic effects, such as oxygen consumption and extracellular lactate levels, and protein-level effects, including the signaling pathways, were all investigated. A functional investigation revealed that metformin and diclofenac combined treatment had synergistic anti-migratory and anti-proliferative effects on BTICs and TCs. The signaling pathways could not fully explain the synergistic effects. However, metformin was found to inhibit cellular oxygen consumption while increasing extracellular lactate levels, indicating glycolytic rescue mechanisms. The combined treatment inhibited metformin-induced lactate increase. The combination of metformin and diclofenac may be a promising new treatment for glioblastoma. Combined treatment may reduce the effective doses of individual agents while inhibiting metabolic rescue mechanisms. More research is needed to determine the potential side effects in humans. As a result, the studies ensured that metformin treatment reduced the intake of oxygen while increasing extracellular lactate levels, indicating increased energy generation *via* glycolysis, whereas diclofenac only slightly reduced lactate. Diclofenac reduced extracellular lactate levels less than in previous studies investigating NSAID's inhibition of cellular lactate production. This could be because BTICs are particularly dependent on mitochondrial ATP production in an oxygen-rich cell culture environment.[67]

A potential improvement in the therapeutic efficacy of biguanide metformin hydrochloride loaded in lipid vesicles (MH-LLVs) on alloxan-induced diabetic rats was investigated.[68] Metformin hydrochloride entrapped in lipid vesicles formed by an integrated process of multiple emulsification and solvent evaporation could effectively reduce hyperglycemia in diabetic animals induced with alloxan. This allowed the biochemical biomarkers under investigation to be restored to near-normal levels. This could be due to the improved bioavailability of the metformin entrapped in lipid vesicles *via* sustained drug release. Overall, the MH-LLV presented here appears to be a promising extended-release formulation, with increased bioavailability, sustained release, and improved antihyperglycemic properties.

In terms of glycemic control, the results show that the longer-acting extended-release (XR) and delayed-release (DR) metformin formulations were as effective as immediate-release (IR) formulations, but the longer-acting formulations offer significant advantages.[69] Metformin XR was linked to lower serum LDL cholesterol levels, whereas metformin DR was strongly linked to lower GI side effects, which may improve drug adherence. More research is needed to fine-tune the optimal cost-benefit ratio of the various metformin preparations available in different clinical settings. Additionally, studies have shown that in patients with diabetes mellitus (DM) treated with insulin and without it, metformin use had no effect on the endothelial healing of drug-eluting stents (DESs). These findings suggest that MF use in these patients should not be discouraged.[70]

3.3.2. Mathematical model for metformin drug release study. To understand the release mechanism of the drugs from the developed Gg-*cl*-poly(AA)/GO (GGAAGO) hydrogels, the drug release kinetics was studied. The metformin hydrochloride drug-release kinetics from the GGAAGO hydrogels can be described using different kinetics models, such as zero order, first order, Higuchi, Hixon–Crowell, and Korsmeyer–Peppas model (see Fig. 5). Therefore, the experimental release data of metformin hydrochloride drug release for the GGAAGO hydrogels were fitted to these models and the related linear regression coefficients (R^2) were obtained. The selected release kinetic model was based on an R^2 value obtained close to unity.[38,39]

Kinetic modeling was performed for all formulations in order to deduce the drug-release mechanism from the developed Gg-*cl*-poly(AA)/GO (GGAAGO) hydrogels, as shown in Table 3. A suitable model was chosen on the basis of the nearness of the "R^2" value to 1. The "R^2" value is the regression coefficient. The "R^2" values of all the models were compared. From Table 3, it could be concluded that the "R^2" value for the Korsmeyer–Peppas model was higher than that for the zero-order, first-order, Higuchi, and Hixson–Crowell models. The release data also showed a good fit with the Korsmeyer–Peppas model. The release exponent "n" value specifies the type of diffusion process, and the "n" values for the developed system of hydrogels were in range of 0.2569–0.4777 (Table 4), confirming anomalous (non-Fickian) diffusion.[71]

The study examined an oral sustained-release (SR) metformin tablet prepared using the direct compression method with hydrophilic hydroxylpropylmethylcellulose (HPMC) and guar gum polymer alone and in combination at various concentrations.[72] The results of the studies revealed that the hydrophilic matrix of HPMC alone could not effectively control metformin release for 12 h, but when combined with guar gum, it could slow the release of the drug and thus be successfully used to formulate SR matrix tablets. Fitting the data to the Korsmeyer equation revealed that diffusion and erosion could be the mechanism of drug release.

3.3.3. Effect of pH on sodium diclofenac drug release. Fig. 6 displays the effect of drug release *versus* time for GGAAGO-0, GGAAGO-1, and GGAAGO-3 hydrogel samples at three different pH values (pH 1.2, pH 7.4, and pH 9.2). An *in vitro* drug-release study was performed for all the samples, GGAAGO-0, GGAAGO-1, and GGAAGO-3 hydrogels at pH 1.2, pH 7.4, and pH 9.2 individually, although a higher percentage release was revealed at pH 9.2 by the created hydrogels compared with at pH 1.2 and 7.4, as exhibited in Fig. 6, while the drug release values (in percentages) are depicted in Table 2. The pH-dependent drug release from the fabricated hydrogels was due to the deprotonation of –COOH groups of gum ghatti and the excess release of carboxylate ions by AA at higher pH, resulting in greater swelling and a greater release of the drug. At pH 9.2, deprotonation of the graphene oxide –COOH groups and excess carboxylate ion released by acrylic acid (pK_a = 4.2) resulted in substantially more expansion and drug release from the manufactured hydrogels, resulting in a higher

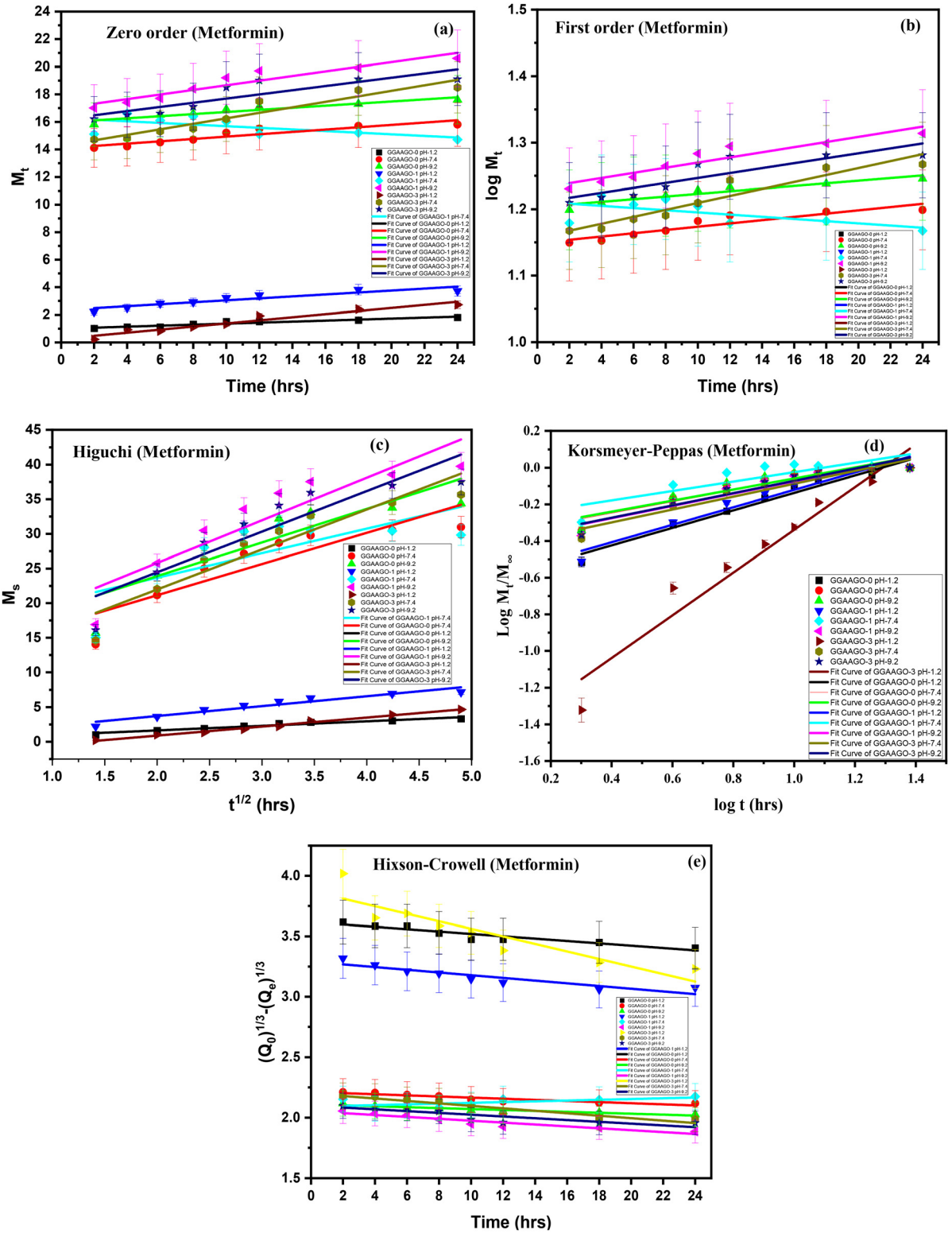

Fig. 5 Dispersed plots for metformin HCl-loaded GGAAGO-0, GGAAGO-1, and GGAAGO-3 hydrogels for different models: (a) zero order, (b) first order, (c) Higuchi, (d) Korsmeyer–Peppas, and (e) Hixson–Crowell.

increase in drug release. The swelling of the created nanocomposite hydrogels was pH dependent, since acrylic acid, graphene oxide, and the hydrogel network all contained different functional groups. Because of the high concentration of –COOH in an acidic environment, the GGAAGO hydrogels did not grow appreciably.

Table 3 Metformin HCl and sodium diclofenac drug-release kinetics of GGAAGO-0, GGAAGO-1, and GGAAGO-3 at different pH values (pH 1.2, pH 7.4, and pH 9.2)

Kinetic models	Zero-order	First-order	Higuchi	Korsmeyer–Peppas		Hixson–Crowell
	M_t *vs.* t	$\log M_t$ *vs.* t	M_t/M_∞ *vs.* $t^{1/2}$	$\log(M_t/M_\infty)$ *vs.* $\log t$		$\sqrt[3]{Q_0} - \sqrt[3]{Q_t}$ *vs.* t
Linear fit	R^2	R^2	R^2	R^2	n	R^2
Metformin hydrochloride						
GGAAG0-0 (pH 1.2)	0.89702	0.85654	0.93444	0.95645	0.47770 ± 0.0384	0.87093
GGAAG0-0 (pH 7.4)	0.84492	0.8383	0.75779	0.85027	0.30998 ± 0.04856	0.84054
GGAAG0-0 (pH 9.2)	0.89189	0.88128	0.72468	0.8255	0.30225 ± 0.05175	0.88487
GGAAG0-1 (pH 1.2)	0.83892	0.79934	0.91292	0.93853	0.47695 ± 0.04592	0.81394
GGAAG0-1 (pH 7.4)	0.27902	0.28444	0.46644	0.64848	0.25695 ± 0.06889	0.28263
GGAAG0-1 (pH 9.2)	0.88103	0.86811	0.80348	0.87824	0.33596 ± 0.04682	0.8725
GGAAG0-3 (pH 1.2)	0.93018	0.67084	0.98671	0.93464	1.16606 ± 0.11597	0.79276
GGAAG0-3 (pH 7.4)	0.89952	0.8936	0.86873	0.91791	0.35195 ± 0.03953	0.89568
GGAAG0-3 (pH 9.2)	0.72684	0.7231	0.8045	0.88214	0.33605 ± 0.04599	0.72436
Sodium diclofenac						
GGAAG0-0 (pH 1.2)	0.8758	0.6091	0.97562	0.92326	1.17765 ± 0.12758	0.72344
GGAAG0-0 (pH 7.4)	0.9687	0.93492	0.9377	0.9525	0.45793 ± 0.03851	0.94783
GGAAG0-0 (pH 9.2)	0.59963	0.56914	0.83601	0.89807	0.48667 ± 0.06148	0.57991
GGAAG0-1 (pH 1.2)	0.73381	0.05439	0.91863	0.93105	0.70432 ± 0.07207	0.66871
GGAAG0-1 (pH 7.4)	0.03628	0.28444	0.61557	0.72665	0.44628 ± 0.10078	0.04887
GGAAG0-1 (pH 9.2)	0.74084	0.7253	0.83489	0.90053	0.38498 ± 0.04798	0.73069
GGAAG0-3 (pH 1.2)	0.90263	0.86693	0.8887	0.92566	0.42423 ± 0.04518	0.8796
GGAAG0-3 (pH 7.4)	0.94365	0.90868	0.95472	0.96296	0.48346 ± 0.03574	0.92179
GGAAG0-3 (pH 9.2)	0.95811	0.92178	0.91344	0.93677	0.43477 ± 0.04249	0.93515

Table 4 Korsmeyer–Peppas model drug release mechanism

Exponent (n)	Drug release mechanism
$n \leq 0.45$	Fickian diffusion (case I diffusional)
$0.45 < n < 0.89$	Anomalous (non-Fickian) diffusion
$n = 0.89$	Zero order release (case II transport)
$n > 0.89$	Super case II transport

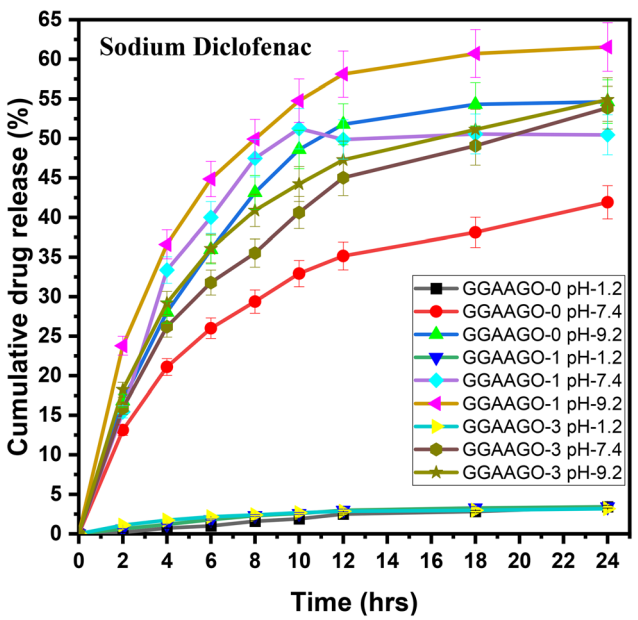

Fig. 6 Plots of cumulative drug release against time (hours) for sodium diclofenac-loaded GGAAGO-0, GGAAGO-1, and GGAAGO-3 hydrogels at pH 1.2, pH 7.4, and pH 9.2 and 37 °C.

The effect of metformin, either alone or in combination with the two nonsteroidal anti-inflammatory drugs (NSAIDs) diclofenac and diflunisal on acute myeloid leukemia (AML) cell lines and primary patient blasts was investigated. Diclofenac, but not diflunisal, decreased lactate secretion in three different AML cell lines (THP-1, U937, and KG-1), and both drugs increased respiration at low concentration. Despite these metabolic effects, both NSAIDs had only a minor effect on tumor cell proliferation and viability up to a concentration of 0.2 mM. At higher concentrations of 0.4–0.8 mM, diflunisal alone had a clear effect on AML cell line proliferation and inhibited respiration. A single dose of the anti-diabetic drug metformin inhibited mitochondrial respiration but did not affect proliferation or viability. However, combining all three drugs resulted in strong cytostatic and cytotoxic effects on THP-1 cells. Similar to the findings with THP-1 cells, the combination of all three drugs significantly reduced primary leukemic blast proliferation and induced apoptosis. Furthermore, the NSAIDs enhanced the effect of low-dose chemotherapy with cytarabine by inhibiting the proliferation of primary AML cells. Together, we show that low concentrations of metformin and the two NSAIDs diclofenac and diflunisal had a synergistic inhibitory effect on AML proliferation and induced apoptosis, most likely by blocking tumor cell metabolism. Our findings demonstrate the feasibility of using anti-metabolic drugs for AML treatment.[73]

Six microparticle formulations (MF-1 to MF-6) made of polyethylene glycol-6000 (PEG-6000) with and without chitosan were loaded with two drugs (DS and SM) using the cold/hot (melt) dispersion method.[74] The formulated microparticles were then mixed with carbopol gel (0.75%–1.00% w/v) and

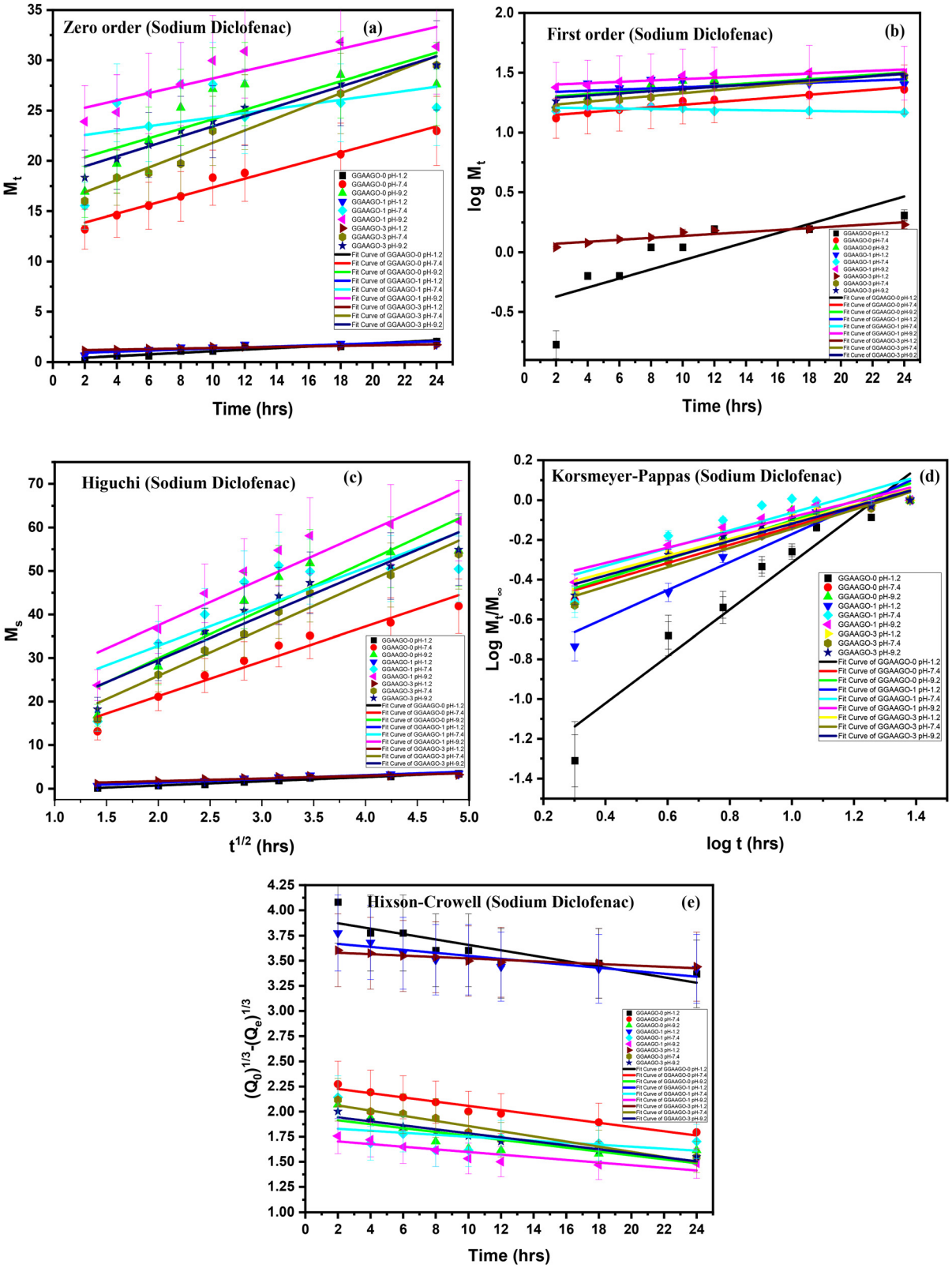

Fig. 7 Dispersed plots for sodium diclofenac-loaded GGAAGO-0, GGAAGO-1, and GGAAGO-3 hydrogels for different models: (a) zero order, (b) first order, (c) Higuchi, (d) Korsmeyer–Peppas, and (e) Hixson–Crowell.

tested. The percentage yield for all the formulated microparticles ranged from 94.13% to 97.18%. The drug contents of both DS and SM were within the permitted limits. The *in vitro* drug-release results showed that the release of DS and SM from the prepared microparticles increased in the chitosan-containing preparation compared to the non-chitosan preparation. When compared to the microparticles alone, the gel formulations showed slower drug release. Based on the findings, it is possible to conclude that chitosan increased the particle size, which led to a faster drug release. The study also suggests that when DS and SM are administered together in pure, microparticle, or gel form, they produce a synergistic drug release effect.

3.3.4. Mathematical model for sodium diclofenac drug-release study. The release data were fitted into different kinetic models. Working equations of these models are stated in Table 3. Fig. 7 shows the fitting efficiency of the kinetic data into these models. The respective regression values and release exponents are reported in Table 3. It was found that the data comply with the Korsmeyer–Peppas (K–P) model best.

Different kinetic models, such as zero order, first order, Higuchi, Hixson–Crowell, and Korsmeyer–Peppas, were used to analyze the drug-release mechanism from the GGAAGO hydrogels by fitting the release data in respective models, as shown in Table 3.[75] The release data exhibited a close fit to the Korsmeyer–Peppas model, which explains the "*n*" diffusion exponent that determines the drug-release mechanism from the developed hydrogels, with the *n* value determining the type of diffusion; whereby $n \leq 0.45$ refers to Fickian diffusion while $0.45 \leq n \leq 0.89$ determines non-Fickian (anomalous) transport, analogous to coupled diffusion/polymer relaxation.[24] The (R^2) values of the Korsmeyer–Peppas model were found to be higher compared to all the other models and were in the range of 0.7266–0.9629. The (*n*) values for all the formulations were in the range of 0.3849–0.7043, as shown in Table 4, representing a non-Fickian diffusion-transport mechanism.

4. Conclusions

In this study, a novel pH-sensitive Gg-*cl*-poly(AA)/GO composite hydrogel was successfully prepared using MBA and TEMED as cross-linkers and APS as an initiator *via* a free-radical-polymerization process. The synthesized hydrogels were well characterized through FTIR and SEM. The *in vitro* drug-release profile revealed the ability of the synthesized hydrogels to extend the drug release for 24 h. The hydrogels were found to be a good drug-delivery systems for the tested drugs in alkaline pH. The release of metformin hydrochloride and sodium diclofenac as a model drugs from hydrogels was observed to be greater at pH 9.2 compared to that at pH 1.2 and pH 7.4. The release mechanism was studied by fitting the experimental data to model equations and calculating the corresponding parameters, and the findings indicated the maximum drug release was at pH 9.2 compared to pH 1.2 and pH 7.4, due to the fact that at pH 9.2, the deprotonation of graphene oxide –COOH groups and excess carboxylate ion released by acrylic acid (pK_a = 4.2) resulted in substantially more expansion and drug release from the manufactured hydrogels, resulting in a higher increase and drug release, allowing the hydrogel to swell further; so more dissolution media entered the hydrogel and enabled further drug release. Both the sodium diclofenac- and metformin-loaded hydrogels followed a non-Fickian transport mechanism. The results demonstrated that the synthesized hydrogels combinations have potential as possible agents for controlled drug-delivery vehicles when quick release of the drug is required at the beginning and controlled release at the end.

Conflicts of interest

There is no conflicts of interest to declare.

References

1 K. A. Rose, D. Lee and R. J. Composto, *Soft Matter*, 2021, **17**, 2765–2774.
2 S. Ullah, Z. Ali, A. S. Khan, A. Nasrullah, F. Javed, B. Adalat, N. Sher, M. Ahmed, R. A. Alshgari, M. S. S. Mushab and S. Majeed, *Chemosphere*, 2024, **356**, 142015.
3 P. Matricardi, C. D. Meo, T. Coviello, W. E. Hennink and F. Alhaique, *Adv. Drug Delivery Rev.*, 2013, **65**, 1172–1187.
4 Y. Wang, J. Wang, Z. Yuan, H. Han, T. Li, L. Li and X. Guo, *Colloids Surf., B*, 2017, **152**, 252–259.
5 O. Ozay, S. Ekici, Y. Baran, S. Kubilay, N. Aktas and N. Sahiner, *Desalination*, 2010, **260**, 57–64.
6 B. A. Getachew, S. R. Kim and J. H. Kim, *Environ. Sci. Technol.*, 2017, **51**, 905–913.
7 K. Sharma, V. Kumar, B. Chaudhary, B. S. Kaith, S. Kalia and H. C. Swart, *Polym. Degrad. Stab.*, 2016, **124**, 101–111.
8 D. Schmaljohann, *Adv. Drug Delivery Rev.*, 2006, **58**, 1655–1670.
9 V. Singh, A. Tiwari, D. N. Tripathi and R. Sanghi, *Carbohydr. Polym.*, 2004, **58**, 1–6.
10 S. Pandey, E. Makhado, S. Kim and M. Kang, *Environ. Res.*, 2023, **217**, 114909.
11 S. Pandey, S. Kim, Y. S. Kim, D. Kumar and M. Kang, *Environ. Res.*, 2024, **240**, 117540.
12 V. Gomase, P. Doondani, D. Saravanan, S. Pandey and R. Jugade, *Sep. Purif. Technol.*, 2024, **330**, 125475.
13 P. Laurienzo, *Mar. Drugs*, 2010, **8**, 2435–2465.
14 J. Sun and H. Tan, *Materials*, 2013, **6**, 1285–1309.
15 S. R. Shin, B. Aghaei-Ghareh-Bolagh, T. T. Dang, S. N. Topkaya, X. Gao, S. Y. Yang, S. M. Jung, J. H. Oh, M. R. Dokmeci, X. Tang and A. Khademhosseini, *Adv. Mater.*, 2013, **25**, 6385–6391.
16 F. Xu, F. Inci, O. Mullick, U. A. Gurkan, Y. Sung, D. Kavaz, B. Li, E. B. Denkbas and U. Demirci, *ACS Nano*, 2012, **6**, 6640–6649.
17 C. Zhang, H. Subramanian, J. J. Grailer, A. Tiwari, S. Pilla, D. A. Steeber and S. Gong, *Polym. Adv. Technol.*, 2009, **20**, 742–747.

18 N. Khanna, T. Chatterji, S. Singh and S. Pandey, *J. Drug Delivery Sci. Technol.*, 2023, **88**, 104958.
19 G. Mustafa, D. Hassan, G. Ruiz-Pulido, M. Pourmadadi, M. M. Eshaghi, R. Behzadmehr, F. S. Tehrani, A. Rahdar, D. I. Medina and S. Pandey, *J. Drug Delivery Sci. Technol.*, 2023, **84**, 104494.
20 I. Rania, A. Anjan, T. K. Sur and B. Piyali, *Res. J. Biotechnol.*, 2021, **16**, 48–57.
21 P. N. Dave, P. M. Macwan and B. Kamaliya, *Colloids Surf., A*, 2023, **673**, 131815–131826.
22 V. Puri, A. Sharma, P. Kumar, I. Singh and K. Huanbutta, *ACS Omega*, 2021, **6**, 15844–15854.
23 P. N. Dave, P. M. Macwan and B. Kamaliya, *Mater. Adv.*, 2023, **4**, 2971–2980.
24 M. Suhail, P. C. Wu and M. U. Minhas, *J. Saudi Chem. Soc.*, 2021, **25**, 101212.
25 N. Orakdogen and B. Sanay, *J. Appl. Polym. Sci.*, 2018, **135**, 45889.
26 K. Sharma, V. Kumar, B. S. Kaith, V. Kumar, S. Som, A. Pandey, S. Kalia and H. C. Swart, *New J. Chem.*, 2015, **39**, 3021–3034.
27 H. Mittal, A. Al Alili, P. P. Morajkar and S. M. Alhassan, *Int. J. Biol. Macromol.*, 2021, **167**, 1248–1261.
28 A. Olad and Z. Rahmani, *Polym. Bull.*, 2023, **80**, 4117–4138.
29 B. S. Kaith, Saruchi, R. Jindal and M. S. Bhatti, *Soft Matter*, 2012, **8**, 2286–2293.
30 Saruchi, M. Kaur, V. Kumar, A. A. Ghfar and S. Pandey, *Polymers*, 2022, **14**, 1911.
31 C. I. Idumah, F. U. Iwuchukwu and J. E. Ogbu, *Inorg. Chem. Commun.*, 2023, **158**, 111640.
32 M. Pourmadadi, M. M. Eshaghi, M. Shaghaghi, S. S. Das, R. Arshad, S. Ghotekar, A. Rahdar, A. L. E. Manicum and S. Pandey, *Open Nanomed. J.*, 2023, **13**, 100175.
33 Z. Nagy, B. Gunay, C. Miller, J. Hahn, M. Ouf, B. W. Hobson, T. Abuimara, K. Bandurski, M. André, L. Lorenz, S. Crosby, B. Dong, Z. Jiang, Y. Peng, M. Favero, J. Y. Park, K. Nweye, P. Nojedehi, H. Stopps, L. Sarran, C. Brackley, K. Bassett, K. Govertsen, N. Koczorek, E. Casavant, M. Kane, Z. O. Neill, T. Yang, J. Day, R. T. Hellwig and M. Vellei, *Build. Environ.*, 2023, 110518.
34 K. Yang, L. Feng, X. Shi and Z. Liu, *Chem. Soc. Rev.*, 2013, **42**, 530–547.
35 X. Yang, X. Zhang, Z. Liu, Y. Ma, Y. Huang and Y. Chen, *J. Phys. Chem. C*, 2008, **112**, 17554–17558.
36 L. Zhang, J. Xia, Q. Zhao, L. Liu and Z. Zhang, *Small*, 2010, **6**, 537–544.
37 S. Rassi and R. Baharfar, *Polyhedron*, 2019, **174**, 114153.
38 M. Nadeem, J. Li, M. Yahya, M. Wang, A. Ali, A. Cheng, X. Wang and C. Ma, *Int. J. Mol. Sci.*, 2019, **20**, 799.
39 M. Xie, H. Lei, Y. Zhang, Y. Xu, S. Shen, Y. Ge, H. Li and J. Xie, *RSC Adv.*, 2016, **6**, 9328–9337.
40 H. Bao, Y. Pan, Y. Ping, N. G. Sahoo, T. Wu, L. Li, J. Li and L. H. Gan, *Small*, 2011, **7**, 1569–1578.
41 M. Nurunnabi, K. Parvez, M. Nafiujjaman, V. Revuri, H. A. Khan, X. Feng and Y. K. Lee, *RSC Adv.*, 2015, **5**, 42141–42161.
42 S. Goenka, V. Sant and S. Sant, *J. Controlled Release*, 2014, **173**, 75–88.
43 P. N. Dave, P. M. Macwan and B. Kamaliya, *Int. J. Biol. Macromol.*, 2023, **224**, 358–369.
44 M. Ubaid and G. Murtaza, *Int. J. Biol. Macromol.*, 2018, **114**, 1174–1185.
45 R. R. Bhosale, R. A. M. Osmani, A. S. Abu Lila, E. S. Khafagy, H. H. Arab, D. V. Gowda, M. Rahamathulla, U. Hani, M. Adnan and H. V. Gangadharappa, *RSC Adv.*, 2021, **11**, 14871–14882.
46 P. B. Aielo, F. A. Borges, K. M. Romeira, M. C. R. Miranda, L. B. D. Arruda, P. N. Paulo, B. D. C. Drago and R. D. Herculano, *Mater. Res.*, 2014, **17**, 146–152.
47 N. S. Barakat and A. A. E. Ahmad, *J. Microencapsulation*, 2008, **25**, 31–45.
48 L. Ali, S. Tanzil, U. Rehman and M. Khan, *Polym. Bull.*, 2019, 3921–3935.
49 E. Makhado, S. Pandey and J. Ramontja, *Int. J. Biol. Macromol.*, 2018, **119**, 255–269.
50 B. Sharma, S. Thakur, D. Trache, H. Y. Nezhad and V. K. Thakur, *Nanomaterials*, 2020, **10**, 1–22.
51 F. Martínez-Gómez, J. Guerrero, B. Matsuhiro and J. Pavez, *Int. J. Biol. Macromol.*, 2018, **111**, 935–946.
52 R. Das and S. Pal, *Colloids Surf., B*, 2013, **110**, 236–241.
53 D. Das, R. Das, P. Ghosh, S. Dhara, A. B. Panda and S. Pal, *RSC Adv.*, 2013, **3**, 25340–25350.
54 D. Das, R. Das, J. Mandal, A. Ghosh and S. Pal, *J. Appl. Polym. Sci.*, 2014, **131**, 1–12.
55 S. Sethi, B. S. Kaith, M. Kaur, N. Sharma and S. Khullar, *J. Biomater. Sci., Polym. Ed.*, 2019, **30**, 1687–1708.
56 Y. L. Ding, Z. Tian, H. J. Li and X. M. Wang, *New Carbon Mater.*, 2019, **34**, 315–324.
57 S. Yadav, A. Asthana, A. K. Singh, R. Chakraborty, S. S. Vidya, A. Singh and S. A. C. Carabineiro, *Nanomaterials*, 2021, **11**, 1–25.
58 A. S. Deshmukh, C. M. Setty, A. M. Badiger and K. S. Muralikrishna, *Carbohydr. Polym.*, 2012, **87**, 980–986.
59 H. Mittal, A. Maity and S. S. Ray, *J. Phys. Chem. A*, 2015, **119**, 2026–2039.
60 P. Rani, G. Sen, S. Mishra and U. Jha, *Carbohydr. Polym.*, 2012, **89**, 275–281.
61 T. Zhang and X. Sun, *Int. J. Nanomater. Nanotechnol. Nanomed.*, 2020, **6**, 1–5.
62 B. Li, C. Wu, C. Wang, Z. Luo and J. Cao, *J. Appl. Polym. Sci.*, 2020, **137**, 1–9.
63 E. Makhado, S. Pandey, P. N. Nomngongo and J. Ramontja, *J. Colloid Interface Sci.*, 2018, **513**, 700–714.
64 D. Delivery, A. Mahmood, A. Erum, U. R. Tulain, S. Shafiq, N. S. Malik, M. T. Khan and M. S. Alqahtani, *Gels*, 2023, **9**, 474–497.
65 M. Z. I. Khan, H. P. Štedul and N. Kurjaković, *Drug Dev. Ind. Pharm.*, 2000, **26**, 549–554.
66 S. Oh, O. Kwon, B. Chun, J. Cho and J. Park, *Fibers Polym.*, 2009, **10**, 21–26.
67 V. Gerthofer, M. Kreutz, K. Renner, B. Jachnik, K. Dettmer, P. Oefner, M. J. Riemenschneider, M. Proescholdt, A. Vollmann-Zwerenz, P. Hau and C. Seliger, *Int. J. Mol. Sci.*, 2018, **19**, 2586.

68 E. C. Ossai, A. C. Madueke, B. E. Amadi, M. O. Ogugofor, A. M. Momoh, C. O. R. Okpala, C. A. Anosike and O. U. Njoku, *Int. J. Mol. Sci.*, 2021, **22**, 1–16.
69 C. Aiken, J. Tarry-Adkins, I. Grant, R. Reynolds and S. Ozanne, *Diabetes Ther.*, 2021, **12**, 2813–2816.
70 H. Cubero-Gallego, R. Romaguera, J. Gómez-Lara, J. A. Gómez-Hospital, M. Sabaté, E. Pinar, M. Gracida, G. Roura, J. L. Ferreiro, L. Teruel, C. Tebé-Codorni, P. Jiménez-Quevedo, E. Montanya, F. Alfonso and Á. Cequier, *Rev. Esp. Cardiol.*, 2018, **71**, 917–925.
71 M. Suhail, A. Khan, J. M. Rosenholm, M. U. Minhas and P. C. Wu, *Gels*, 2021, **7**, 1–16.
72 K. Wadher, M. Umekar and R. Kakde, *Int. J. Pharm. Invest.*, 2011, **1**, 157.
73 K. Renner, A. Seilbeck, N. Kauer, I. Ugele, P. J. Siska, C. Brummer, C. Bruss, S. M. Decking, M. Fante, A. Schmidt, K. Hammon, K. Singer, S. Klobuch, S. Thomas, E. Gottfried, K. Peter and M. Kreutz, *Front. Pharmacol.*, 2018, **9**, 1–13.
74 T. R. Sekharan, S. Tamilvanan, S. C. Rajesh and J. Jenishiya, *Lett. Appl. NanoBioScience*, 2023, **12**, 111.
75 K. Ghosal, A. Das, S. K. Das, S. Mahmood, M. A. M. Ramadan and S. Thomas, *Int. J. Biol. Macromol.*, 2019, **130**, 645–654.